New Method for Analysis of Nanoparticle Geometry in Supported fcc Metal Catalysts with Scanning Transmission Electron Microscopy

Anna Carlsson, Anna Puig-Molina, and Ton V. W. Janssens*

Haldor Topsøe A/S, Nymøllevej 55, DK-2800 Lyngby, Denmark

Received: November 30, 2005; In Final Form: January 31, 2006

To apply the knowledge of reaction mechanisms of heterogeneously catalyzed reactions on the atomic scale to supported catalyst systems, a detailed description of the structure of active particles on the atomic scale is required. In this article, a method is developed to construct atomic-scale geometric models for supported active fcc metal nanoparticles, based on a measurement of particle sizes and particle volumes by Scanning Transmission Electron Microscopy (STEM) and the M−M coordination number determined from EXAFS. The method is applied to supported Au/TiO_2, $Au/MgAl_2O_4^-$, and Au/Al_2O_3 catalysts. These geometric models allow for estimation of geometric properties, such as specific Au surface area, metal−support contact perimeter, metal−support contact surface area, edge length, and number of Au atoms located at the corners of the particles, with an error on the order of 20%. In the three catalysts studied here we find that the Au particles in the Al_2O_3 supported catalyst are small. The Au particles in the Au/TiO_2 catalyst are smaller in diameter than those for the $Au/MgAl_2O_4$, but also thicker. The differences in particle size and shape seem to reflect the differences in the metal−support interface energy in the three catalyst systems.

1. Introduction

The fundamental knowledge about heterogeneously catalyzed reactions has increased significantly in the past decades, and the elucidation of reaction mechanisms plays a central role in this development. In several cases, a reaction mechanism on the atomic scale has been constructed, e.g. for ammonia synthesis[1] or the MoS_2-catalyzed hydrodesulfurization (HDS) reaction,[2] which correlates the detailed structure of the catalyst with catalytic activity. The active sites in a catalyst typically consist of several atoms in a very specific configuration. For example, in the Ru-catalyzed ammonia synthesis, an arrangement of 5 Ru atoms on a step edge seems to be responsible for the dissociation of the N_2.[3] For the MoS_2-catalyzed hydrodesulfurization reaction, the special configuration of the sulfur atoms at the edges of MoS_2 crystallites seems to be responsible for the catalytic activity.[2,4,5]

The conclusions about the active site are usually based on a detailed characterization of model systems, which is often combined with quantum-chemical calculations. However, supported catalysts, which are usually applied in industry, are complex systems that are much less uniform, and not as well defined as the model systems. To apply the knowledge about the reaction mechanisms and the structure of the active sites to the performance of supported catalysts, a more detailed atomic-scale description of the structure in such catalysts is required. Such a description may consist of how many occurrences of a given geometry are present in the catalysts, e.g., the number of 5 Ru-atom ensembles per gram of catalyst in a Ru-based catalyst for ammonia synthesis, or the total edge length in a MoS_2-based hydrotreating catalyst.[2,4]

In many cases, atomic-scale structural information in industrial catalysts is difficult to obtain. Zeolite-based catalysts are probably the easiest to study: The structure of the active (acid) site is given by the crystal structure of the zeolite, and the number of acid sites can be obtained by measurement of the adsorption capacity of base molecules, e.g., ammonia or pyridine. In the structurally more complex supported metal catalysts, the relevant quantities such as metal−support interface edge length, or the density of a site with a specific geometry are often estimated from an average particle size or particle size distribution.[6] Usually, rather simple models are used to describe the particle geometry, e.g., hemispheres with a diameter equal to an average diameter obtained by chemisorption or X-ray diffraction. However, as this is not necessarily the correct geometry of the active particles, such a geometric model may result in significant errors.

In this paper, we present a new method based on scanning transmission electron microscopy (STEM) with a High Angle Annular Dark Field (HAADF) detector to construct a more accurate geometric model of the metal particle shapes for supported fcc metal catalysts, by example, of Au/TiO_2, $Au/MgAl_2O_4$, and Au/Al_2O_3 catalysts. The Au-based catalysts are chosen because Au gives a good contrast in HAADF-STEM, and the particles are therefore easy to analyze. Furthermore, the geometry of the Au particles is crucial for the catalytic properties: The activity can vary by several orders of magnitude, just dependent on the size and possibly the shape of the Au particles.[7−12] Therefore, the results of this study contribute to the understanding of structural and particle-size effects in Au catalysts. This paper is confined to the derivation of the geometric properties of the supported Au particles; the relation between the structure of the Au particles and catalytic activity is beyond the scope of the present article.

The geometry of the individual Au particles is estimated from a measurement of both particle size distributions and the volume of the individual Au particles with HAADF-STEM, and the Au−Au coordination number as determined from EXAFS. The volume of the Au particles is derived from the intensity in the HAADF-STEM images.[13] By combining a measured particle

* Corresponding author. E-mail: tvj@topsoe.dk.

10.1021/jp0569537 CCC: $33.50
Published on Web 03/01/2006

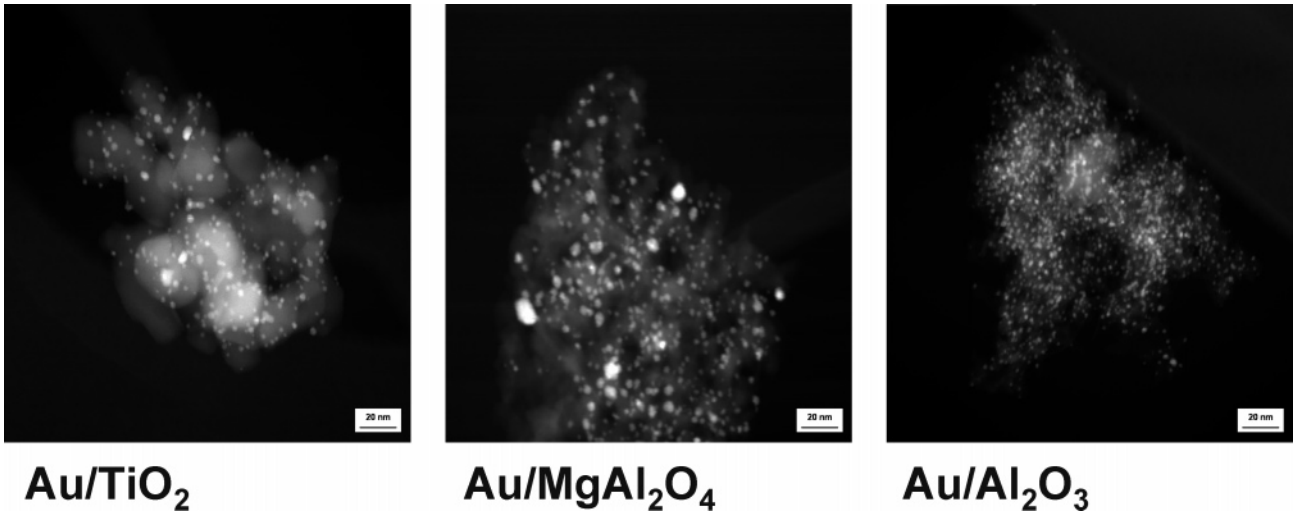

Figure 1. Scanning transmission electron microscopy (STEM) images of Au/TiO_2 (4.4 wt % Au), $Au/MgAl_2O_4$ (4.1 wt % Au), and Au/Al_2O_3 catalysts (4.0 wt % Au).

size and particle volume, a three-dimensional model particle is constructed. The final geometric model then consists of a set of these model particles, with a size and volume distribution that matches the experimentally determined one, a total gold volume that corresponds to the gold content in the catalysts, and a Au−Au coordination number that matches the values determined by separate EXAFS measurements. These structural models for the supported metal particles constitute a basis to obtain more accurate estimates of geometric properties, such as specific surface area or number of atoms at edges, corners, or other specific sites, which allows for a more accurate estimation of the active site density of the supported catalysts.

2. Experimental Section

The supported gold catalysts used in this study are Au/TiO_2, $Au/MgAl_2O_4$, and Au/Al_2O_3. These catalysts were prepared by homogeneous deposition precipitation of Au on the support material. The Au content in these catalysts, determined by ICP-OES, is 4.4 wt % in the Au/TiO_2 catalyst, 4.1 wt % in the $Au/MgAl_2O_4$ catalyst, and 4.0 wt % in the Au/Al_2O_3 catalyst. Prior to the STEM measurements, the catalyst samples are activated in a quartz U-tube reactor by heating for 1 h at 400 °C in a mixture of 1% CO, 21% O_2, and 78% Ar at atmospheric pressure. After the activation, the catalysts were exposed to the same gas mixture for an additional 10−15 h at 0 °C. Then the samples were taken out of the reactor and transferred to the electron microscope under inert atmosphere.

The HAADF-STEM measurements were performed on a Philips CM200 transmission electron microscope, with an electron energy of 200 keV. The STEM images were obtained by focusing the electron beam to a diameter of about 5 Å, at a scanning speed of 60 s/image, which is sufficient to measure Au particles as small as 7 Å. For the construction of the particle geometry, a large number of particles must be measured; a typical number of particles measured in the experiments here is on the order of 2000. Furthermore, as the measured intensity in the STEM images is used, it is very important that the pixel resolution in the images is smaller than the spot size, and that all images within a series are recorded at the same brightness and contrast settings to make a proper comparison between different images possible.

The Au−Au coordination number was determined from separate EXAFS measurements with a fresh sample of the same catalyst batches. These measurements were performed at beamline X1 of the HASYLAB synchrotron in transmission mode, using a double Si(111) crystal monochromator. The catalyst samples were placed in a reactor cell with full control of gas atmosphere and temperature. The catalysts were heated for 1 h at 400 °C in a mixture of 1% CO, 21% O_2, and 78% Ar, which is the same pretreatment as used in the microscopy measurements. After this activation, the EXAFS spectra at the Au−L_3 edge from which the Au−Au coordination numbers were derived were obtained at 25 °C under the same gas atmosphere. The Au−Au coordination numbers (N) were corrected for inharmonic effects by using $N_{corr} = N_{measured} + 36T\alpha(12 - N_{measured})$,[14] where T is the temperature in the EXAFS experiment and α is the linear expansion coefficient for gold (14.2×10^{-6} K^{-1}).

3. Construction of the Model Particle Geometries

The construction of a three-dimensional model of the individual Au particles in the Au/TiO_2, $Au/MgAl_2O_4$, and Au/Al_2O_3 catalysts requires information on (1) Au particle sizes, (2) Au particle volumes, and (3) total Au content in the catalyst. The Au particle sizes and volumes are derived from HAADF-STEM measurements.

A typical HAADF-STEM image of the three Au catalysts is given in Figure 1. The contrast in HAADF-STEM is obtained by differences in the current of electrons that are deflected to an angle between 4° and 10° at different locations in the sample. The deflected current is proportional to the number of atoms in the beam, multiplied by an atom-specific cross section for electron scattering.[13] As a consequence, the intensity in the STEM images becomes proportional to the number of atoms at a specific location, if all particles have the same chemical composition. The cross section for scattering increases approximately with the square of the atom number (Z^2), which results in a high intensity for areas with a high concentration of heavy atoms. This means that the Au atoms appear as bright spots in the STEM image, while the support, which contains much lighter elements, is gray.

The first step in the construction of a geometric model of the gold particles is to derive a particle size distribution for the Au particles, which is readily available from the STEM images. In the analysis, only particles appearing as round ($P^2/4\pi A < 1.05$, where P is the perimeter and A is the area of the particle in the STEM image) are used in the analysis to avoid particles imaged edge-on, and accidental overlap of particles at different

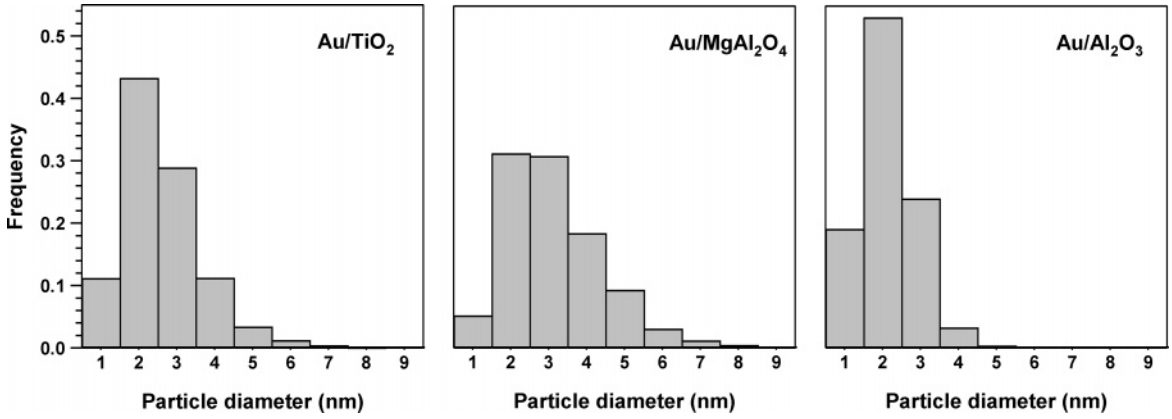

Figure 2. Particle size distributions of the Au/TiO_2, $Au/MgAl_2O_4$, and Au/Al_2O_3 catalysts derived from a series of STEM images.

heights in the sample. In the particle size distributions, an averaged particle diameter is used, which is calculated from the measured area as $d = (4A/\pi)^{1/2}$. Figure 2 shows the particle size distributions for the Au/TiO_2, $Au/MgAl_2O_4$, and Au/Al_2O_3 catalysts used in this study, based on analysis of about 2000 particles in each catalyst. The particle size in the three catalysts is quite different: The average Au particle diameters are 2.1, 3.5, and 1.6 nm for the Au/TiO_2, $Au/MgAl_2O_4$, and Au/Al_2O_3, respectively; the corresponding standard deviation of the particle size distributions is 1.1, 2.5, and 0.7 nm.

The next step is to determine how the volume of the individual gold particles changes with the diameter. To achieve this, we use the property that the intensity in the STEM images is proportional to the number of atoms in the beam, as explained above. First the intensity due to the Au particles alone is estimated by subtraction of the contribution of the support—the gray background—from the intensity in the bright areas (Au particles). The integrated intensity over the whole particle then is proportional to the total number of gold atoms in that particle, or the particle volume.

Figure 3 shows a double-logarithmic plot of the measured integrated intensities as a function of the measured particle diameters (in nm) for the three catalysts studied here. The scattering of the data points for particles larger than approximately 2 nm indicates that the volume of the particles with a given diameter varies in a narrow range, which indicates that the particle heights at a given diameter are very similar. For very small particles the scattering in the data becomes larger, which is probably a reflection of the accuracy of the measurement: Very small particles are hard to distinguish in the images, and the relative error made by the background subtraction will be larger as well. The solid lines, which have a slope of 2 (left) and 3 (right), are drawn as a guide to the eye, and indicate that the measured curves are slightly concave.

To convert the measured particle size and particle volume distributions to a geometric model for the particles in the catalysts two assumptions are needed. The first assumption is that the measured distributions are representative for the entire sample. This assumption is usually tacitly made in microscopy, but we use it here in a more explicit way: The total integrated intensities of all particles measured in the STEM images corresponds to the total number of gold atoms (or volume of gold) per gram of catalyst.

The second assumption required for the construction of a geometric model of the Au particles is a basic particle geometry. The size and volume of this geometry is then varied according to the distributions measured in HAADF-STEM. In the analysis presented here, we have used the top slice of a truncated octahedron, with the (111) facets parallel to the surface of the support. The truncated-octahedral geometry is compatible with the fcc structure of the Au particles[15] and the regular polyhedron that is the best approximation of the Wulff reconstruction for gold. The parameters that are independently varied are the number of atoms at the edge (m) and the number of atomic layers in the slice (l). Figure 4 shows an example of a model particle that has 4 atoms at the edges and 5 layers ($m = 4$, $l = 5$). The Wulff reconstruction of the Au particles probably does not have a constant edge length; this simplification is made here to make the geometric model more manageable.

The final step is to convert the integrated particle intensities, which are only a relative measure of the particle volumes, to absolute particle volumes. If we can assign a known volume or height to a particle of a given diameter, then the volumes and heights of all other particles can be determined form the data in Figure 3, and an estimate of the particle geometries can be obtained. To be able to do so, additional information on the particle geometry is needed to obtain an estimate for the absolute particle volumes. This additional information must come from an independent method, and can, for instance, be an average coordination number obtained by EXAFS, or a specific surface area from chemisorption measurements. For the Au/TiO_2, $Au/MgAl_2O_4$, and Au/Al_2O_3 catalysts discussed here, we have used a Au−Au coordination number from EXAFS measurements.

By combining the information from the experimentally determined particle size distribution, particle volumes, and the Au−Au coordination numbers obtained by EXAFS, we have constructed the geometric model for the Au particles as follows. First, we calculate the average Au−Au coordination number for different assumptions for the height of a particle with a diameter of 2 nm. Reasonable values for this height will lie in the range 0.3−1.2 nm, which corresponds to 1−5 atomic layers. These calculated Au−Au coordination numbers for the Au/TiO_2, $Au/MgAlO_4$, and Au/Al_2O_3 catalysts result in the curves shown in Figure 5. By matching the calculated coordination number with the measured values, one obtains an estimate for the height, and volume, of a particle with a diameter of 2 nm, from which the final geometric model can be constructed. Note that this procedure is equivalent to adjust the volume−intensity conversion factor in order to fit the measured Au−Au coordination numbers. A particle with a diameter of 2 nm that is approximately 5 layers thick for the Au/TiO_2 and the $Au/MgAl_2O_4$ catalysts and 3 layers thick for the Au/Al_2O_3 matches the EXAFS data best, and that set is chosen as the geometric model for the Au nanoparticles in the catalysts.

Using the known particle diameters and volumes, a value for the edge length and the number of layers can be determined

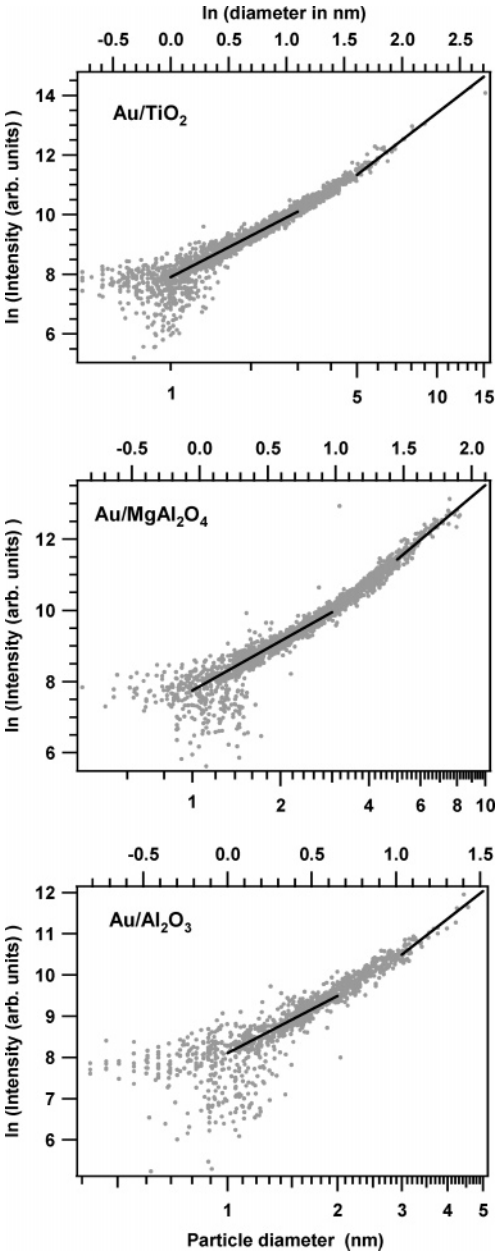

Figure 3. Double-logarithmic plot of the measured integrated intensity in the STEM images as a function of the measured particle size for each individual Au particle in the Au/TiO_2, $Au/MgAlO_4$, and Au/Al_2O_3 catalysts. The integrated intensity is proportional to the number of Au atoms, or volume, of the Au particles. The solid lines have a slope of 2 (left) and 3 (right); they indicate a transition from 2-D to 3-D particle growth in the range 3−5 nm. The solid lines are a guide to the eye.

for each particle, using the geometric formulas that are available in the Supporting Information to this article. This results in a set of model particles with the same size and volume distribution as determined from the STEM measurement. The final geometric model consists of the distribution of the particles over the edge lengths (m) and thicknesses (l).

The set of model particles derived above is consistent with the measured particle size distributions, particle volumes, and EXAFS coordination numbers. The distribution of Au particle geometry in the three catalysts is given in Table 1 and represented in Figure 6. This is used as a basis for calculations of the geometric properties of the gold particles in these catalysts. The area of the circles in the graphs in Figure 6 is proportional to the percentage of particles with the given edge length and number of layers. The differences in geometry

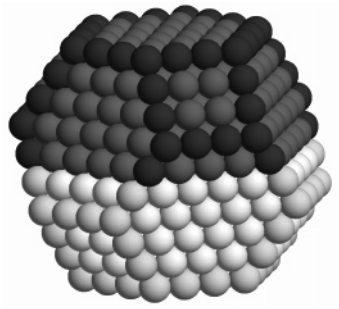

Figure 4. The basic truncated octahedral particle geometry that is used to construct the geometric models for the gold particle. The dark part represents the geometry of a particle with 4 atoms at the edge and 5 atom layers thick ($m = 4$, $l = 5$).

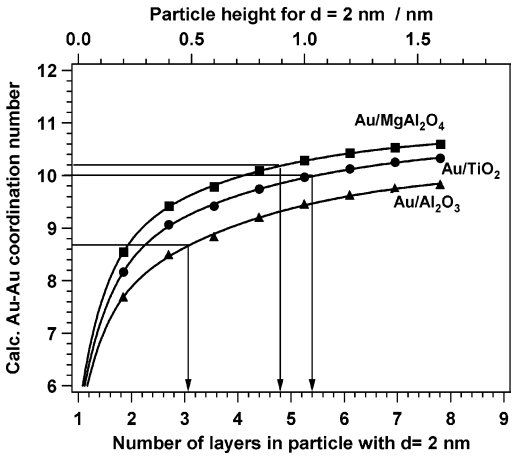

Figure 5. Calculated Au−Au coordination number, using the geometric models, as a function of the assumed height for a particle with a diameter of 2 nm for the Au/TiO_2, $Au/MgAl_2O_4$, and Au/Al_2O_3 catalysts. A particle height of 5.4, 4.8, and 3.1 nm for the Au/TiO_2, $Au/MgAl_2O_4$, and Au/Al_2O_3, respectively, results in the coordination numbers that match those measured by EXAFS.

between the three catalysts are quite clear; Au/Al_2O_3 has many small particles (edge length 2 or 3), while a significant part of the Au particles of both the Au/TiO_2 and $Au/MgAl_2O_4$ catalysts are larger, with an edge length up to 5 atoms. In addition, the Au particles in the Au/TiO_2 catalysts are clearly thicker and rounder, compared to the $Au/MgAl_2O_4$ catalyst, with up to 6 layers at an edge length of 4 atoms.

An overview of several structural properties estimated on the basis of the geometric models for the Au/TiO_2, $Au/MgAl_2O_4$, and Au/Al_2O_3 catalysts is given in Table 2. The numbers in brackets indicate the percentage of Au atoms that are located in that specific position, which is a reflection of the dispersion of the Au particles on the different support materials. Clearly, the Au/Al_2O_3 catalyst has the highest dispersion, as also can be seen directly in the STEM images. The added value of the method presented above is that it quantifies how many atoms are in specific locations in a supported catalyst. This information is indispensable for application of the fundamental knowledge about the surface chemistry of Au obtained from surface spectroscopic studies or theoretical calculations to complex, supported catalysts.

4. Discussion

The geometric models for the Au particles in the supported catalysts depend on the measurement of the volume of each Au particle by STEM, using a proportionality between the intensity in STEM and number of atoms in the sample. Such a

TABLE 1: Distribution of the Au Particles in the Au/TiO_2, $Au/MgAl_2O_4$, and Au/Al_2O_3 Catalysts over the Edge Length and Number of Layers in the Slices of the Truncated Octahedra[a]

number of layers (l)	edge length (m)											
	2	3	4	5	6	7	8	9	10	11	12	13
						Au/TiO_2						
1	-	0.17										
2	0.67	0.38										
3	4.26	0.33										
4	17.07	0.42										
5		9.27	8.14	1.42	0.13	0.13						
6		17.53	15.19	8.18	1.88	0.54	0.13	0.08	0.08	0.04		
7		2.34	1.42	3.38	2.17	1.13	0.29	0.13	0.04			
8			0.04	0.25	0.50	0.58	0.33	0.25	0.13	0.08		
9				0.04	0.04	0.08	0.08					
10						0.04	-	0.17		0.04	0.04	
11						0.04	0.04	0.04			0.04	
12							0.04					0.04
13										0.04		
						$Au/MgAl_2O_4$						
1	-	0.04	0.18									
2	0.27	1.15	0.09									
3	1.77	1.24	0.04									
4	10.12	0.97	0.49	0.09	0.04	0.04						
5		10.70	16.22	5.70	0.97	0.40	0.18					
6		6.54	5.35	11.63	3.93	1.24	0.27	0.13	0.04			
7		0.88	0.27	1.90	5.35	2.03	0.49	0.18				
8			0.04	0.04	1.11	2.21	0.62	0.09				0.04
9					0.04	0.57	0.84	0.35	0.04		0.04	
10			0.04		0.04	0.31	0.22	0.49	0.04		0.04	0.04
11					0.04		0.18	0.35	0.18	0.04		
12						0.04	0.13	0.18	0.13	0.13		
13				0.04					0.04	0.09		
14								0.09	0.04			
						Au/Al_2O_3						
1	0.35	2.30	-	0.09								
2	2.93	3.37	0.27	-								
3	10.90	20.30	14.89	6.65	3.10	0.35	0.09					
4	14.98	7.45	4.43	4.70	1.60	0.44	0.18					
5	-	0.18	0.18				0.09					
6	-	0.09	-			0.09						

[a] The numbers indicate the percentage of the particles that have that particular geometry.

measurement of the particle volume in this way is valid in general, although it has some limitations. The first limitation is that all particles to be studied must have the same chemical composition, but the method is in principle not limited to metal catalysts. For particles with varying composition, such as alloys or mixed oxide catalysts, the determination of the particle volume with STEM requires additional information about the composition of every single particle, and about the electron deflection cross section as a function of the particle composition. This may complicate the analysis significantly.

A second limitation is that the method only can be applied to systems that consist of heavy-element particles on light-element supports. This is an immediate consequence of the fact that the cross section for electron deflection increases with the atomic number, roughly as Z^2. The measured intensity for heavy atoms in the STEM images is much higher than that for the light elements, and as a consequence, a small amount of a lighter element on a heavier support, (e.g., Ni/CeO_2) will be invisible in the STEM images. In the Au/TiO_2, $Au/MgAl_2O_4$, and Au/Al_2O_3 catalysts studied here, the Au yields a good contrast that allows for an accurate determination of the STEM intensities.

The accuracy of the analysis depends on several factors, including the measurement errors in microscopy and EXAFS, the choice of the particle geometry, and the assumption that structural irregularities such as steps and kinks on the particles can be neglected. A well-calibrated electron microscope will typically have a magnification error of less than 10%. For these three samples a 10% error in the measured diameters will change the calculated surface area by 1−5%, depending on the actual particle size distribution. The error in the number of corner sites is larger and is on the order of 20−25%. A 2% error in the EXAFS coordination number, the estimated measurement error, will change the surface areas by 2−5%, and the number of corner sites by 3−12%. This indicates that the error due to such measurement errors is rather limited.

For particle size distributions with long tails at large particle diameters, the failure to include a few large particles can cause rather large errors in the calculated properties. For the Au/TiO_2 sample the two largest particles, out of 2396 particles in total, stand for 6% of the total volume. If these two particles are removed from the particle size distribution, the surface area increases by 3% and the number of corner sites by 2%.

In the construction of the model particles, we have assumed a perfect truncated-octahedral structure. To evaluate the effect of this choice of geometry, we also performed an analysis using cuboctahedral particles, which is another geometry that is compatible with the fcc crystal structure of the Au particles. The solid and dashed lines in Figure 7 show the specific Au area and the number of corner atoms for the Au/TiO_2 obtained with a truncated-octahedral and cubooctahedral geometry, respectively. Clearly, the surface area is not very much affected by the choice of geometry, but the number of corner atoms is

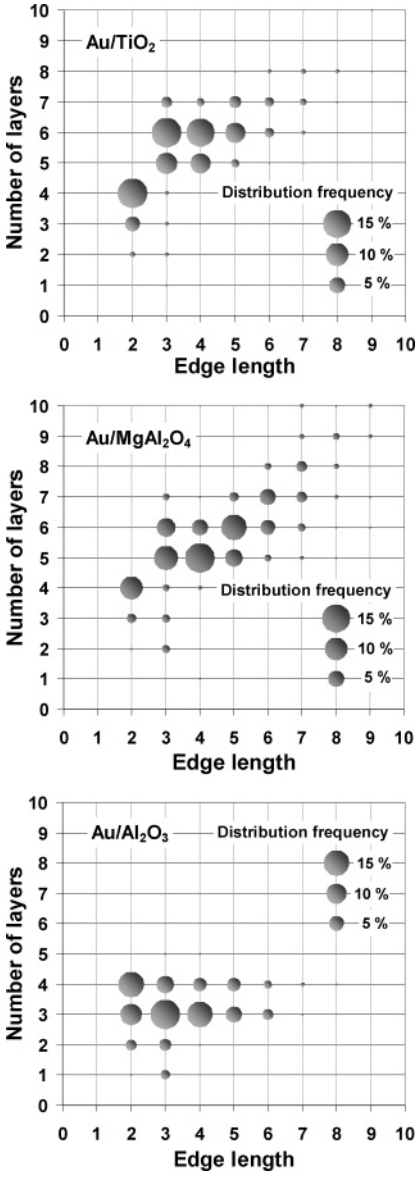

Figure 6. Particle geometry distributions for the Au/TiO_2, $Au/MgAl_2O_4$, and Au/Al_2O_3 catalysts. The area of the circles indicates the fraction of the Au particles with the indicated edge length (horizontal axis) and number of layers (vertical axis).

about 40% lower for cubooctahedral particles. This is primarily a consequence of the fact that a truncated octahedron contains 24 corner atoms, and a cuboctahedron 12.

In the present study, we did not account for the presence of steps and kinks on the small Au particles. However, it is very likely that the Au particles have steps and kinks. A recent study has shown that the presence of CO may induce formation of steps and kinks on a Au surface.[16] A correction for steps and kinks will systematically lead to larger values for the edge length and number of corner atoms; the surface area is not very much affected by the presence of extra steps and kinks. However, the effect of these geometric irregularities is expected to be limited to about 20%. This can be seen as follows: a perfect particle has 12 corner atoms, addition of a step to a particle leads to 2 extra corner atoms per particle, for larger particles possibly 3 extra corner atoms; the expected error here is also 25% at most. A similar argument can be given for the error induced by neglecting steps: The total edge length on a particle is about 12 times the length of a single edge, or 6 times the particle diameter. If a particle has a step, the total step length on that particle will be approximately equal to the particle diameter. This leads to a total edge length that is 16% higher than that for the perfect geometry. Finally, it should be noted that the errors due to the choice of geometry and structural irregularities tend to cancel when the particle geometries in different catalysts are compared to each other.

An alternative way to estimate geometric properties of nanoparticles from particle size distributions, which does not require the use of measured particle volumes, is to assume a fixed relation between particle diameter and height. The difference with the analysis presented in the previous section is that we have replaced the measured diameter/volume relationship with an estimated one. Two realistic cases are represented by either assuming a constant height, independent of particle diameter, or a height that is proportional to the diameter. The constant height in the first case can be interpreted as an average particle height; the second case corresponds to a constant aspect ratio of the particles. To obtain accurate results, it is required to adjust this height or aspect ratio to fit an independently measurable parameter, which can be the coordination number obtained from EXAFS. This is completely analogous to the procedure used to estimate the absolute particle volumes from the STEM intensities. When using hemispheres or spheres, as often is encountered in the literature, the average height or aspect ratio is not adjusted to an independently measurable property, and may therefore result in significant errors.

The symbols in Figure 7 show the results for the specific Au area and the number of corner atoms in the Au/TiO_2 catalyst, which is calculated for particles with a constant average height, with a constant average aspect ratio, and using the measured diameter−volume relationship as a function of the Au−Au coordination number. These data indicate that the error introduced by using a simplified volume−diameter relationship is limited for this particle size distribution, and they therefore can be good alternatives when no particle volume data are available.

The geometry analysis of the Au particles in the previous section revealed that the Au particles on the three supports have a different shape, which is a direct consequence of a different Au/support interface energy in the three catalysts. On the basis of DFT calculations, it has been shown that adhesion of Au on a TiO_2 surface requires an oxygen vacancy,[17] and therefore the interface energy and the final shape of the Au particles depends on the vacancy density in TiO_2. The higher dispersion of the Au on the Au/Al_2O_3 observed in the STEM images in Figure 1 suggests that the interface energy in the Au/Al_2O_3 catalyst is higher. In fact, the estimated thickness of a 2 nm particle on the three different supports, which is indicated in Figure 5, is a measure of the interface energy: the higher the interface energy, the thinner the particle. According to this argument, the trend in the adhesion of energies of the Au particles in the three catalysts studied here is $Au/Al_2O_3 > Au/MgAl_2O_4 > Au/TiO_2$. The high dispersion of the Au particles in the Au/Al_2O_3 catalyst after heating to 400 °C, compared to the $Au/MgAl_2O_4$ and Au/TiO_2 catalysts, points to a higher resistance of the Au particles against sintering, which is in full agreement with the indicated order in the adhesion energy given above.

The measured relationship between the particle volume and diameter, which is displayed in Figure 3, also could be applied to study the growth of the gold particles. The double-logarithmic curves in Figure 3 are slightly concave; the slope varies from approximately 2 for small particles to 3 for the larger particles (>5 nm), as is indicated by the solid lines. Therefore, the volume of the small particles is proportional to d^2 for small particles and to d^3 for large particles. This suggests that the small particles

TABLE 2: Geometric Properties of the Au Particles in the Au/TiO_2, $Au/MgAl_2O_4$, and Au/Al_2O_3 Catalyst, Estimated from the Geometric Models Based on a Truncated Octahedral Particle Geometry, and the Au−Au Coordination Number Measured by EXAFS[a]

geometric property	Au/TiO_2	$Au/MgAl_2O_4$	Au/Al_2O_3
number of particles measured	2396	2262	1128
number of particles per g of catalyst	3.49×10^{17}	2.07×10^{17}	9.67×10^{17}
specific Au surface (m^2/g_{cat})	3.52 (32.5%)	2.91 (28.8%)	4.28 (39.9%)
metal/support contact surface (m^2/g_{cat})	1.51 (18.8%)	1.43 (18.7%)	2.52 (36.8%)
contact perimeter (m/g_{cat})	2.28×10^9 (5.9%)	1.80×10^9 (5.0%)	5.26×10^9 (14.9%)
edge length (not in contact with support) (m/g_{cat})	7.59×10^9 (10.7%)	5.34×10^9 (8.0%)	13.7×10^9 (17.0%)
number of Au corners per g of catalyst	7.11×10^{18} (5.6%)	3.92×10^{18} (3.4%)	15.5×10^{18} (14.1%)
Au−Au coordination no. measured by EXAFS	10	10.2	8.7

[a] The numbers in parentheses indicate the fraction of Au atoms in the catalyst in that specific configuration, and reflect the dispersion of the gold in the three catalysts.

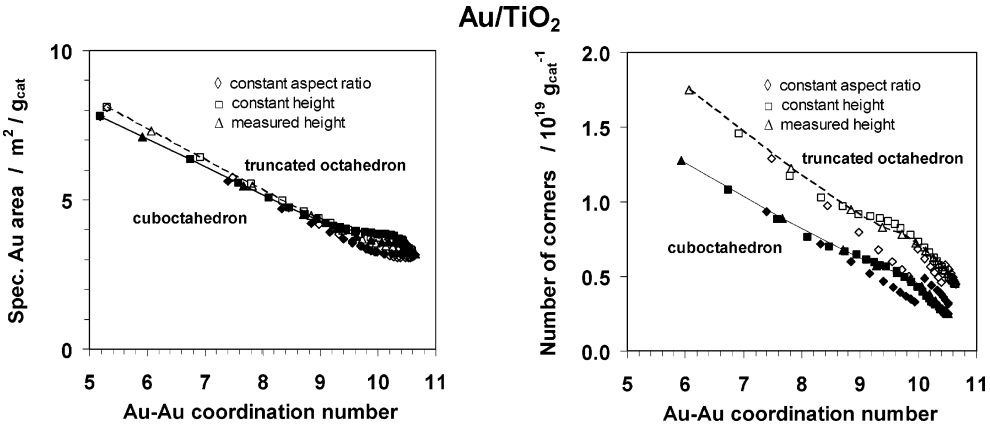

Figure 7. Influence of the choice of basic particle geometry and height−diameter relationship on the estimated specific Au surface area and number of Au atoms located at the corners of the Au particles in the Au/TiO_2 catalyst. The dashed lines and open symbols indicate the results obtained with a truncated octahedron; the solid lines and filled symbols are obtained assuming a cuboctahedral geometry for the Au particles. Diamonds: Results obtained under the assumption of constant aspect ratio (h/d). Squares: Results obtained under the assumption of a constant particle height (h). Triangles: Results obtained from the measured relationship between particle volume and diameter.

grow two-dimensionally, which implies that the height of the particles does not change significantly in this size range. The large particles grow three-dimensionally, and have therefore a constant aspect (height/diameter) ratio. The transition from two-dimensional to three-dimensional growth takes place in the range 3−5 nm, in the catalysts studied here. The fact that the majority of the Au particles in the Au/TiO_2 catalyst are in the 2-D growth regime also explains why the approximation with a constant average height, as shown in Figure 7, agrees better with our measured results, compared to the approximation with a constant aspect ratio.

5. Conclusions

A new method to construct a geometric model for individual supported nanoparticles has been developed, which is based on the simultaneous measurement of particle size and particle volume using Scanning Transmission Electron Microscopy (STEM). This method can be generally applied for heavy-element compounds on light-element supports, under the restriction that particles have a uniform chemical composition and crystal structure that is known, and an appropriate particle shape in the relevant size range can be estimated.

We applied this method to construct geometric models for the Au particles in Au/TiO_2, $Au/MgAl_2O_4$, and Au/Al_2O_3 catalysts. With these geometric models, structural and geometric properties of the supported Au particles on the atomic scale, such as the specific Au surface area, the contact perimeter and area, the total edge length, and the number of Au atoms located at the corners of the Au particles, are estimated with higher accuracy compared to the usually applied sphere or half-sphere models. This makes it possible to obtain a direct count of the number of sites with a certain geometry for samples with different particle size distributions and geometries. The error introduced due to measurement error and the assumption of a perfect particle geometry seems to be limited to approximately 20−25%, and tends to cancel when different catalysts are compared to each other.

If particle volume data are not available, then assuming particles with a constant height or constant aspect ratio can be good alternatives to estimate geometric properties of nanoparticles, provided the height and aspect ratio of the particles is adjusted to an independently measurable property, such as surface area or coordination number.

The geometry of the gold particles in the three catalysts is quite different. As is immediately clear from the STEM images, the Au particles in the Au/Al_2O_3 catalyst are small, compared to the Au/TiO_2 and $Au/MgAl_2O_4$ catalysts. The Au in the $Au/MgAl_2O_4$ catalyst are larger in diameter, but also have generally a more flat geometry than the particles in the Au/TiO_2 catalyst. These differences in Au particle shape reflect differences in Au−support interface energy in the three catalyst systems.

Supporting Information Available: Formulas for the geometric properties of fcc nanoparticles. This material is available free of charge via the Internet at http://pubs.acs.org.

References and Notes

(1) Sehested, J.; Jacobsen, C. J. H.; Törnqvist, E.; Rokni, S.; Stoltze, P. *J. Catal.* **1999**, *188*, 83.

(2) Lauritsen, J. V.; Nyberg, M.; Nørskov, J. K.; Clausen, B. S.; Topsøe, H.; Lægsgaard, E.; Besenbacher, F. *J. Catal.* **2004**, *224*, 94.

(3) Jacobsen, C. J. H.; Dahl, S.; Hansen, P. L.; Törnqvist, E.; Jensen, L.; Topsøe, H.; Prip, D. V.; Møenshaug, P. B.; Chorkendorff, I. *J. Mol. Catal. A* **2000**, *163*, 19.

(4) Lauritsen, J. V.; Bollinger, M. V.; Lægsgaard, E.; Jacobsen, K. W.; Nørskov, J. K.; Clausen, B. S.; Topsøe, H.; Besenbacher, F. *J. Catal.* **2004**, *221*, 510.

(5) Lauritsen, J. V.; Helveg, S.; Lægsgaard, E.; Stensgaard, I.; Clausen, B. S.; Topsøe, H.; Besenbacher, F. *J. Catal.* **2001**, *197*, 1.

(6) Bethke, G. K.; Kung, H. H. *Appl. Catal. A* **2000**, *194*−*195*, 43.

(7) Haruta, M.; Yamada, N.; Kobayashi, T.; Ijima, S. *J. Catal.* **1989**, *115*, 301.

(8) Haruta, M. *Catal. Today* **1997**, *36*, 153.

(9) Haruta, M.; Tsubota, S.; Kobayashi, T.; Kageyama, H.; Genet, M. J.; Delmon, B. *J. Catal.* **1993**, *144*, 175.

(10) Valden, M.; Lai, X.; Goodman, D. W. *Science* **1998**, *281*, 1647.

(11) Lai, X.; St. Clair, T. P.; Valden, M.; Goodman, D. W. *Prog. Surf. Sci.* **1998**, *59*, 25.

(12) Lopez, N.; Janssens, T. V. W.; Clausen, B. S.; Xu, Y.; Mavrikakis, M.; Bligaard, T.; Nørskov, J. K. *J. Catal.* **2004**, *223*, 232.

(13) Treacy, M. M. J.; Rice, S. B. *J. Microsc.* (*Oxford, U.K.*) **1989**, *156*, 211.

(14) Clausen, B. S.; Nørskov, J. K. *Top. Catal.* **2000**, *10*, 221.

(15) van Hardeveld, R.; Hartog, F. *Surf. Sci.* **1969**, *15*, 189.

(16) Piccolo, L.; Loffreda, D.; Cadete Santos Aires, F. J.; Deranlot, C.; Jugnet, Y.; Sautet, P.; Bertolini, J. C. *Surf. Sci.* **2004**, *566*−*568*, 995.

(17) Lopez, N.; Nørskov, J. K.; Janssens, T. V. W.; Carlsson, A.; Puig-Molina, A.; Clausen, B. S.; Grunwaldt, J.-D. *J. Catal.* **2004**, *225*, 86.